Effect of Sulfur Deposition on the Horizontal Well Inflow Profile in the Heterogeneous Sulfur Gas Reservoir

Mingren Shao, Qi Yang, Bo Zhou, Shuhui Dai, Ting Li,* and Faraj Ahmad

ACCESS | 📊 Metrics & More | 📖 Article Recommendations

ABSTRACT: A semianalytical coupled reservoir/wellbore model based on the volumetric source for horizontal wells of sulfur gas reservoirs is presented, which considers sulfur deposition and permeability heterogeneity. Compared to the results without considering the sulfur deposition effect, the results of this paper model is better fitted to field production data and average relative errors of two simulated results are 8.37% (considering sulfur deposition) and 23.38% (not considering sulfur deposition). Based on the model, we perform sensitivity in terms of various sulfur depositions, producing pressure drop, and permeability contrast. Results show that the production decreases with increased sulfur deposition, and the flow rate along the wellbore in the horizontal well decreases because of sulfur deposition. The production without and with sulfur deposition increases with increased producing pressure drop, while the production without sulfur deposition is higher. Also, higher producing pressure drop causes a higher nonuniform inflow profile along the horizontal well. Sulfur deposition can reduce a nonuniform biased inflow profile along the horizontal well in heterogeneous sulfur gas reservoirs, but the horizontal well production is reduced. Therefore, sulfur deposition is crucial for the production prediction and inflow profile along the horizontal well in heterogeneous sulfur gas reservoirs.
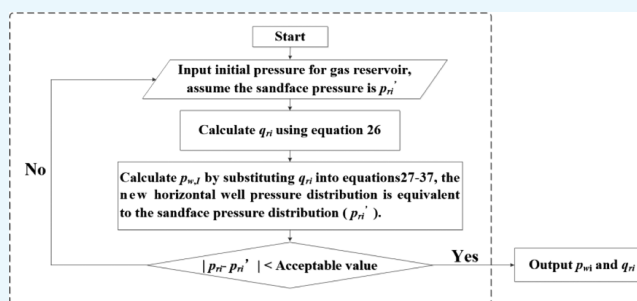
INTRODUCTION

Sulfur deposition has attracted increasing attention because it harms production in sulfur gas reservoirs. Sulfur deposition tends to occur when the temperature and pressure of high sulfur gas reservoirs change. The gas reservoir pressure drops, as the gas production increases; hence, sulfur saturation in the sulfur gas decreases.[1−6] Based on sulfur saturation, some mathematical models were built to predict the influence of sulfur deposition on the gas inflow profile of horizontal wells,[7−9] but these models are based on vertical wells. Furthermore, few researchers are concerned about the horizontal well inflow profile in heterogeneous sulfur gas reservoirs.

Over the past few decades, many researchers have focused on horizontal well oil/gas inflow along the horizontal wells,[10−12] and this problem involves complex reservoir seepage, wellbore flow, and their relationship.[13−20] Penmatcha and Aziz[15] and Ozkan et al.[16] developed reservoir/well models by the point source function to predict the flow rate and pressure distribution along the horizontal wellbore, and the point source function was also widely used for transient pressure analysis in other gas reservoirs such as the coalbed methane gas reservoir,[17−19] but the solution of the point source function has the characteristic of singularity.[20] Vicente et al.[21] developed a three-dimensional implicit simulator to solve the coupling equation between the reservoir and wellbore. The numerical model can be used to analyze the flow rate and pressure distribution of horizontal

wells accurately and deeply, and they need more data and more computation time than analytical solution and semi-analytical solution. Ouyang and Huang[22] presented a coupled reservoir/wellbore model using experimental results, but did not consider porous media seepage in the reservoir. Karimifard and Durlofsky[23] proposed a new method to consider the interaction between a wellbore model and a reservoir model. However, the boundary conditions in the wellbore model are constants, and this leads to erroneous results in applications.

Souza et al.[24] proposed a numerical model to simulate the coupling of the wellbore and reservoir, which takes into account factors such as wellbore length, isotropy and anisotropy, completion scheme, and formation damage near the wellbore area. However, this method needs longer computational time than the analytical method and semianalytical method.[25−28] The volumetric source method[25] was proposed to evaluate the inflow profile for horizontal well completion with inflow control devices, and computational efficiency and high accuracy were

obtained. The reservoir/well model of Furui was improved by Adesina et al.,[29] who considered the pressure drop caused by acceleration. However, the influence of formation damage near the well area has not been effectively solved. Moreover, less attention was focused on the effects of sulfur deposition on the horizontal well inflow profile in the heterogeneous sulfur gas reservoir.

In this study, a new reservoir/wellbore coupling model using the volumetric source method is presented to evaluate the effect of sulfur deposition on the horizontal well inflow profile in the heterogeneous sulfur gas reservoir. Also, the sensitivity factors such as sulfur deposition, producing pressure drop, and permeability contrast are studied. This work provides a method to predict gas production and evaluate the effect of sulfur deposition on the horizontal well inflow profile in the heterogeneous sulfur gas reservoir.
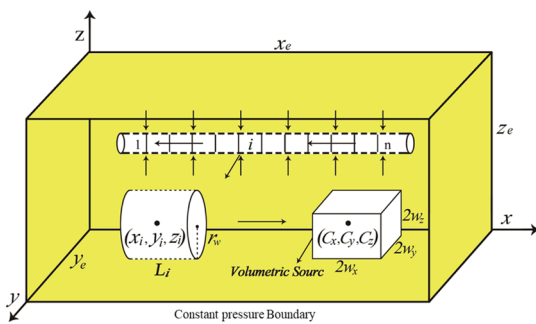

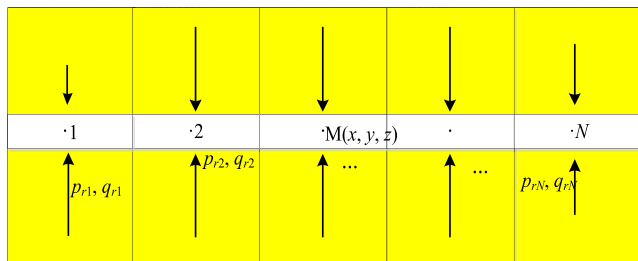**Figure 1.** Schematic diagram of the box gas reservoir and horizontal well.

Figure 2. Schematic of the horizontal well and gas reservoir division.
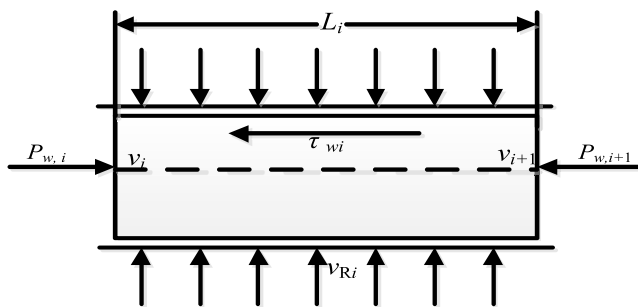

Figure 3. Flow model in the horizontal wellbore.

Sulfur Deposition Damage Model. For sulfur gas reservoir development, the main effects of sulfur deposition are the decrease of the porosity and the decrease of the permeability. It is assumed that the pressure change in time d_t is d_p and the change in sulfur solubility is d_C. During the d_t time, the volume of the precipitated solid sulfur in the saturated gas stream is given as follows
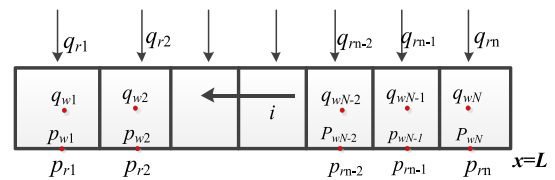

Figure 4. Coupling diagram of gas reservoir seepage and wellbore flow.
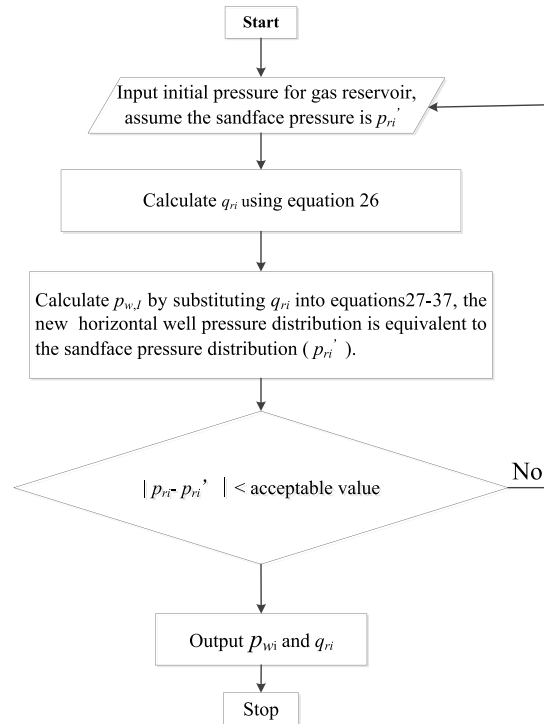

Figure 5. Calculation flow chart for the model.

$$d_{V_s} = qB_g d_C d_t = qB_g (d_C/d_p)_T d_t/\rho_s \tag{1}$$

where V_s is the precipitated sulfur volume (m³); q is the flow rate (m³); B_g is the gas volume factor (m³/m³); C is the sulfur solubility in gas (g/m³); p is the reservoir pressure (MPa); t is the production time (d); T is the gas reservoir temperature (K); and ρ_s is the density of the solid sulfur (2.07 g/cm³).

The deposition amount of the sulfur element in the reservoir can be calculated by eq 1. The deposited solid sulfur clogs the rock pores, and so, the relationship between porosity changes and time can be expressed as[30]

$$\phi = \phi_0 - \frac{1}{a} \ln\left(1 + \frac{amq^2}{h^2 r^2} t\right) \tag{2}$$

where $m = ((d_C/d_p)_T \mu_g B_g 2/k_0)$. where ϕ is the porosity after sulfur deposition, which is dimensionless; ϕ_0 is the initial porosity, which is also dimensionless; a is the laboratory coefficient, and its empirical value is -6.842; h is the net thickness (m); r is the sulfur deposition radius (m); μ_g is the gas viscosity (mPa·s); and k_0 is the initial permeability ($10^{-3} \mu m^2$).

The relationship between sulfur deposition saturation and porosity is given as

$$\phi d_{S_s} = -d_\phi \tag{3}$$

where S_s is sulfur deposition saturation.

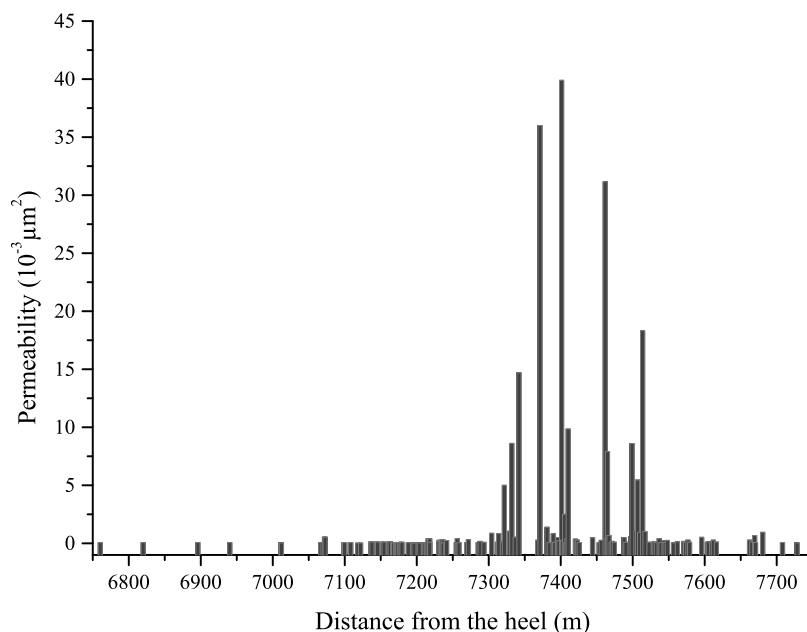By integrating eq 3, sulfur saturation can be expressed as

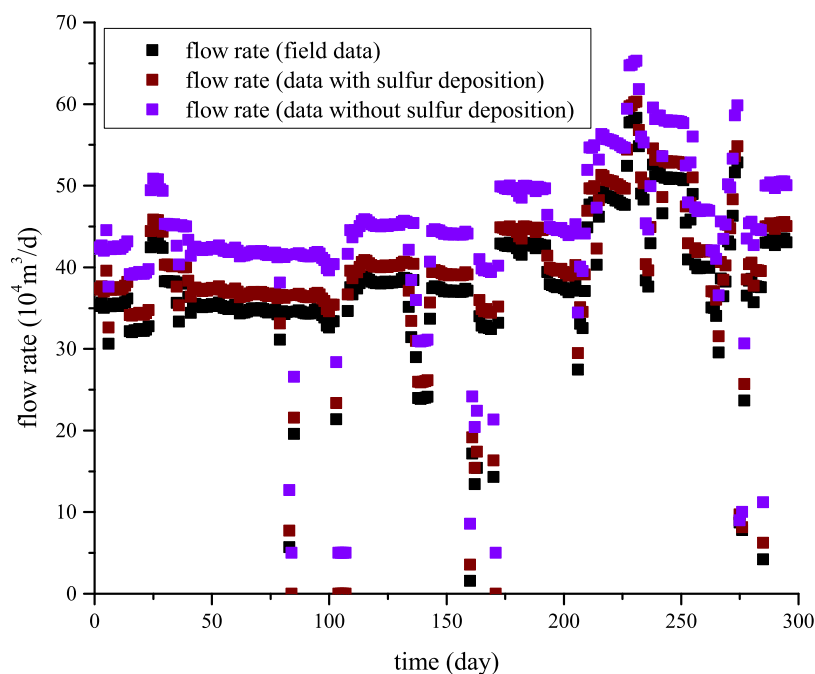**Figure 6.** Permeability along the horizontal well.

Figure 7. Comparison to field data.

$$S_s = \ln \frac{\phi_0}{\phi} \qquad (4)$$

Sulfur deposition affects not only saturation but also the formation permeability. Based on the results reported by Robert,[9] the formation permeability and the sulfur deposition saturation can be expressed as

$$\ln \frac{k}{k_0} = aS_s \qquad (5)$$

where k is the permeability after sulfur deposition ($10^{-3} \, \mu m^2$).

Therefore, the permeability after sulfur deposition can be expressed as

$$k = k_0 e^{aS_s} \qquad (6)$$

■ SEMIANALYTICAL MODEL AND SOLUTION

Assumptions. As we can see in Figure 1, the sulfur gas reservoir is assumed to be a homogeneous reservoir. The gas reservoir (big box) and volumetric source (small box) are shaped as a cuboid box. There are five closed boundaries and one constant pressure boundary on the big box. The surface of the source (small box) is parallel to the gas reservoir. The horizontal well exists in the middle of the big box and fully penetrates the sulfur gas reservoir. It is assumed that the flow in the sulfur gas reservoir is a single steady flow, and the gas flow

conforms to Darcy's law. Sulfur is precipitated in the form of elementary substances during the production process.

Reservoir Flow Model. As shown in Figure 1, the sulfur gas reservoir model is described by the following parameters: the sizes of the sulfur gas reservoir are x_e, y_e, and z_e. In the heterogeneous sulfur gas reservoir, the gas production intensity of a volume source is q. The sizes of the volumetric source are $2w_x$, $2w_y$, and $2w_z$ in three directions, and the center coordinate is $(c_x,\ c_y,\ c_z)$. Based on the abovementioned assumption, the diffusion equation of the gas flow in the sulfur gas reservoir can be expressed as

$$\frac{\partial^2(\psi)}{\partial x^2} + \frac{\partial^2(\Delta\psi)}{\partial y^2} + \frac{\partial^2(\Delta\psi)}{\partial z^2} + \frac{\mu_g q_{gsc} p_{gsc} T}{86.4 k_0 e^{aS_s} V_{source} T_{sc}}$$

$$h(x,\ y,\ z) = 0 \qquad (7)$$

Boundary conditions

$$\left.\frac{\partial(\Delta\psi)}{\partial x}\right|_{x=0, x=x_e} = 0 \qquad (8)$$

$$\left.\frac{\partial(\Delta\psi)}{\partial y}\right|_{y=0, y=y_e} = 0 \qquad (9)$$

$$\left.\frac{\partial(\Delta\psi)}{\partial z}\right|_{z=z_e} = 0 \qquad (10)$$

$$\Delta\psi|_{z=0} = 0 \qquad (11)$$

where

$$\psi = 2\int_{P_{gsc}}^{P_i} \frac{p}{\mu Z}\,dp \qquad (12)$$

$$\Delta\psi = \psi_i - \psi_g \qquad (13)$$

$$V_{source} = 8w_x w_y w_z \qquad (14)$$

$$h(x,\ y,\ z) = [H(x - c_x - w_x) - H(x - c_x + w_x)]$$
$$\times [H(y - c_y - w_y) - H(y - c_y + w_y)]$$
$$\times [H(z - c_z - w_z) - H(z - c_z + w_z)] \qquad (15)$$

$H(x - x_0)$ is the Heaviside function

$$H(x - x_0) = \begin{cases} 1 & x > x_0 \\ 0 & x \le x_0 \end{cases} \qquad (16)$$

where ψ_i is the original pseudopressure of the gas reservoir, MPa; ψ_g is the pseudopressure at any point of the sulfur gas reservoir, MPa; q_g is the volumetric source strength of the sulfur gas reservoir, m³/d; V_{source} is the geometry size of the volumetric source, m³; k_0 is the reservoir permeability, μm^2; p is the reservoir pressure at any point of the sulfur gas reservoir, MPa; p_{ini} is the original gas reservoir pressure, MPa; μ_g is the gas viscosity, mPa·s; Z is the deviation factor of the sulfur gas reservoir; p_{sc} is the pressure under surface standard conditions, MPa; T_{sc} is the temperature under surface standard conditions, K; and T is the gas reservoir temperature, K.

The solution of the diffusion equation of the gas flow in the sulfur gas reservoir can be written by eq 16. A detailed derivation process of the solution for the diffusion equation based on the

Table 1. Basic Parameters of the Sulfur Gas Reservoir and Horizontal Well

parameters	value
sulfur gas reservoir length [m]	980
sulfur gas reservoir width [m]	600
top depth of the reservoir [m]	6730.3
porosity[fraction]	0.16
initial pressure [MPa]	70
gas density [kg/m³]	0.69
horizontal well length [m]	980
reservoir thickness [m]	60
horizontal well radius [mm]	120
gas viscosity [mPa·s]	0.026
wellbore roughness [m]	0.04

volumetric source model in this section can be found in the Appendix.[19,20]

$$\Delta\psi = G(\Delta\psi) = \sum_{l=0}^{\infty}\sum_{m=0}^{\infty}\sum_{n=0}^{\infty} \frac{1}{\gamma} \frac{q_{sc} p T}{86.4 k e^{\alpha S_s} V_{source} T_{sc}}$$

$$\frac{-E_{l,m,n}(x,\ y,\ z)G[h(x,\ y,\ z)]}{\|E_{l,m,n}(x,\ y,\ z)\|^2} = \frac{q_{sc} p T}{86.4 k e^{\alpha S_s} V_{source} T_{sc}}$$

$$\sum_{l=0}^{\infty}\sum_{m=0}^{\infty}\sum_{n=0}^{\infty} \frac{\sigma_l(x)\sigma_m(y)\sigma_n(z)}{\gamma} \qquad (17)$$

In this study, the cylindrical horizontal well is equivalent to a rectangle shape (Figure 1). The rectangle is divided into N parts (Figure 2), and each part is regarded as a volumetric sink, the length of part i is L_i, the wellbore radius is r_w, and the coordinates of i is $(x_i,\ y_i,\ z_i)$. Therefore, the coordinates of part i and dimensions of three directions are as follows

$$(c_{xi},\ c_{yi},\ c_{zi}) = (x_i,\ y_i,\ z_i) \qquad (18)$$

$$2w_{xi} = L_{hi} \qquad (19)$$

$$2w_{yi} = 2w_{zi} = \sqrt{\pi r_w^2} \qquad (20)$$

Corresponding to the division of horizontal wells, the gas reservoir is also divided into N parts, as shown in Figure 2. According to the superposition principle, the pressure drop at any point $M(x,y,z)$ in the sulfur gas reservoir is obtained by the following equation

$$\Delta\psi_i = \sum_{i=1}^{N}\left[\frac{q_{sc} p_{sc} T}{86.4 k e^{aS_s} V_{source} T_{sc}} \right.$$
$$\left. \sum_{l=0}^{\infty}\sum_{m=0}^{\infty}\sum_{n=0}^{\infty} \frac{\sigma_{lj}(c_{xi})\sigma_{mi}(c_{yi})\sigma_{ni}(w_{zi} - c_{zi})}{\gamma} \right] \qquad (21)$$

It is assumed that there is no cross flow between the two adjacent sulfur reservoir segments and that the point $M(x,y,z)$ is located in the center of part i. According to eq 21, the pressure drop of point M can be expressed as

$$\Delta\psi_i = \sum_{j=1}^{N}\left[\frac{q_{gsci} p_g T}{86.4 k e^{aS_s} V_{source} T_{sc}} \right.$$
$$\left. \sum_{l=0}^{\infty}\sum_{m=0}^{\infty}\sum_{n=0}^{\infty} \frac{\sigma_{lj}(c_{xi})\sigma_{mj}(c_{yi})\sigma_{nj}(c_{zi} - w_{zi})}{\gamma} \right] \qquad (22)$$
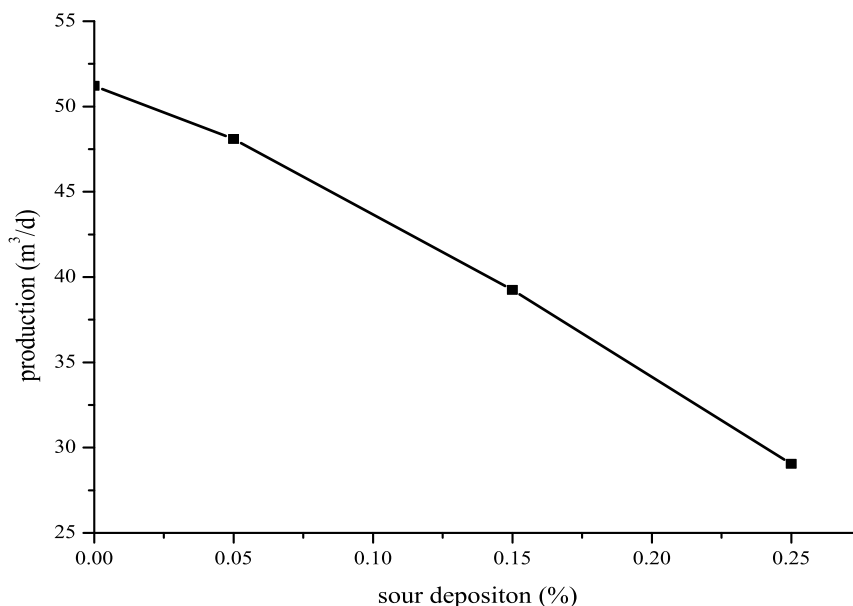
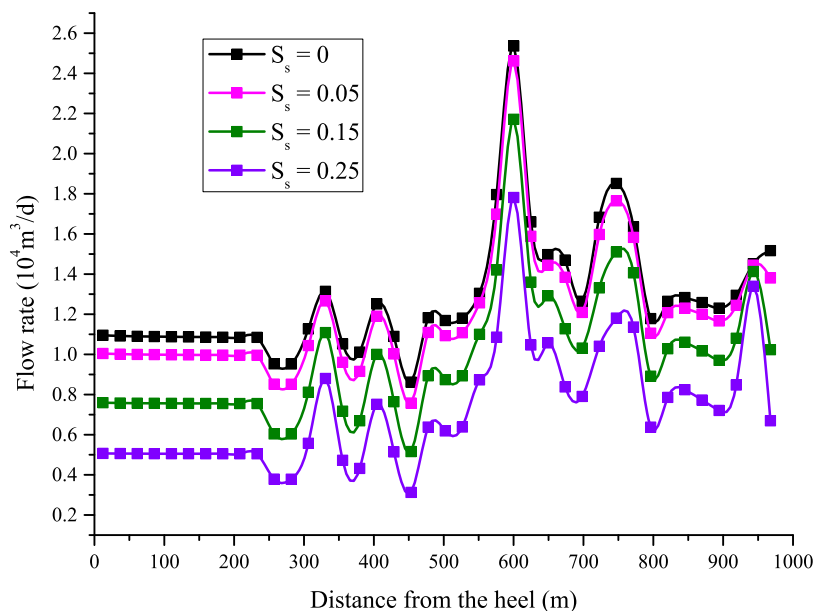**Figure 8.** Production changes with sulfur deposition.

Figure 9. Influence of sulfur deposition.

Eq 13 is substituted into eq 22 to obtain the pressure of part i

$$\psi_g = \psi_i - \sum_{j=1}^{M}\left[\frac{q_{gsci}pT}{86.4kV_{source}T_{sc}}\right.$$
$$\left.\sum_{l=0}^{\infty}\sum_{m=0}^{\infty}\sum_{n=0}^{\infty}\frac{\sigma_{lj}(c_{xi})\sigma_{mj}(c_{yi})\sigma_{nj}(c_{zi}-w_{zi})}{\gamma}\right] \quad (23)$$

The $s-k^*$ approach[31] was presented to model reservoir permeability heterogeneity near the wellbore region. s is a constant background permeability and k^* is the effective skin along the horizontal well. The skin factor caused by the reservoir heterogeneity by Hawkins' method[32] can be expressed as

$$S_{hi} = \left(\frac{k}{k_i} - 1\right)\ln\frac{r_a}{r_w} \quad (24)$$

Substituting the eq 24 into the eq 23, the pressure of part i for the sulfur gas reservoir is

$$\psi_g = \psi_i - \sum_{j=1}^{M}\left[\frac{q_{gsci}pT}{86.4ke^{aS_s}V_{source}T_{sc}}\right.$$
$$\left.\sum_{l=0}^{\infty}\sum_{m=0}^{\infty}\sum_{n=0}^{\infty}\frac{\sigma_{lj}(c'_{xi})\sigma_{mj}(c'_{yi})\sigma_{nj}(w'_{zi}-c'_{zi})}{\gamma}\right]$$
$$-\frac{q_{gsci}pT}{86.4ke^{aS_s}L_{hi}T_{sc}}S_{hi} \quad (25)$$

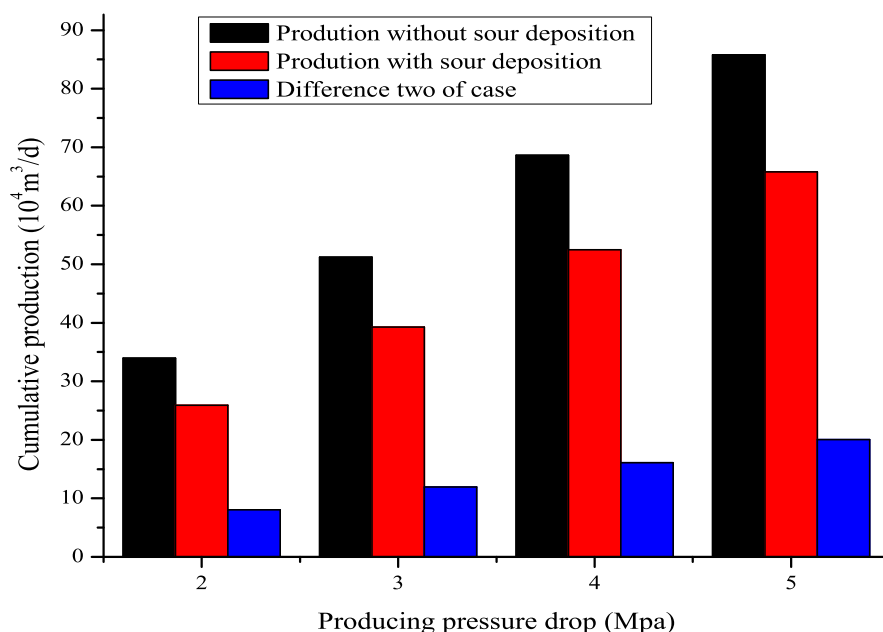Substituting eq 16 into the eq 25, the eq 25 is converted as

Figure 10. Influence of producing pressure drop.

$$p_{ri}^{2} = p_{ini}^{2} - 2\mu \sum_{j=1}^{M} \left[\frac{Z_i q_{gsci} p T}{86.4 k e^{aS_s} V_{source} T_{sc}} \right.$$
$$\left. \sum_{l=0}^{\infty} \sum_{m=0}^{\infty} \sum_{n=0}^{\infty} \frac{\sigma_{lj}(c'_{xi})\sigma_{mj}(c'_{yi})\sigma_{nj}(w'_{zi} - c'_{zi})}{\gamma} \right]$$
$$- \frac{\mu Z_i q_{gsci} p T}{43.2 k e^{aS_s} L_{hi} T_{sc}} S_{hi} \tag{26}$$

Wellbore Flow Model. In this study, a single fluid is assumed to flow between two nodes, as shown in Figure 3. As shown in Figure 3, the mass conservation equation can be expressed as:

$$\rho v_i \frac{\pi D^2}{4} + \rho v_{Ri} \pi D d_{L_i} - \left[\rho v_i + \frac{\partial v_i}{\partial L_i} d_{L_i} \right] \frac{\pi D^2}{4} = 0 \tag{27}$$

According to eq 27, the following equation can be obtained as follows:

$$\frac{\partial v_i}{\partial L_i} = \frac{4 v_{Ri}}{D} \tag{28}$$

The conservation equation can be written as follows:

$$-\frac{d_{P_{w,i}}}{d_x} = 1.0 \times 10^{-6} \left\{ \frac{4\tau_{wi}}{D} + \rho \left[2v_i \frac{\partial v_i}{\partial x} + \left(\frac{\partial v_i}{\partial x} \right)^2 \right] d_{L_i} \right\} \tag{29}$$

Let $\tau_{wi} = \frac{f_i \rho v_i^2}{8}$, and τ_{wi} and eq 28 are substituted into eq 29 to obtain the pressure drop

$$-\frac{d_{P_{w,i}}}{d_{L_i}} = 1.0 \times 10^{-6} \left(\frac{f_i \rho v_i^2}{2D} + \frac{8\rho v_i v_{Ri}}{D} + \frac{16\rho p_{Ri}^2}{D^2} \right) d_{L_i} \tag{30}$$

where the friction coefficient f can be written as[33]

$$f = \begin{cases} \dfrac{64}{R_e} & R_e \leq 2300 \\[2ex] \dfrac{0.3164}{\sqrt[4]{R_e}} & 2300 < R_e < 4000 \\[2ex] \left[1.14 - 2lg\left(\dfrac{\varepsilon}{d} + 21.25 R_e^{-0.9} \right) \right]^{-2} & R_e \geq 4000 \end{cases} \tag{31}$$

The ranges $R_e \leq 2300$, $2300 < R_e < 4000$, and $R_e \geq 4000$ correspond to laminar flow, transition flow, and turbulent flow, respectively.

The properties of the gas (pressure, density, and gas flow rate) by the ideal gas can be expressed as

$$\rho = \frac{M_{air} \gamma_g p}{RTZ} \tag{32}$$

$$v_i = \frac{\rho_{sc} q_{sci} T Z}{p \pi r_w^2 T_{sc}} \tag{33}$$

Assuming that the fluid flow near the wellbore is uniform, the gas velocity of part i from the sulfur gas reservoir to the wellbore can be expressed as

$$v_{Ri} = \frac{p_{sc} q_{sci} T Z}{2 \pi r_w p T_{sc} L_i} \tag{34}$$

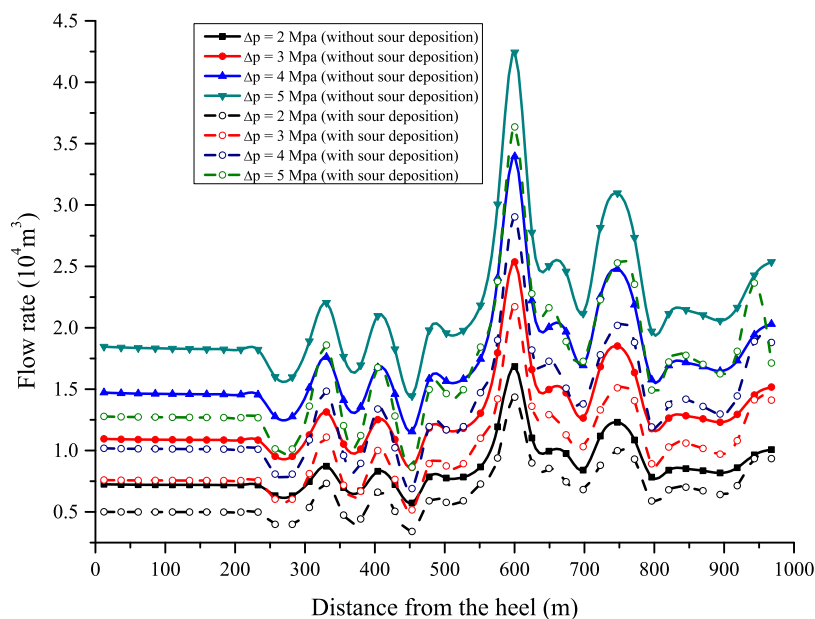From eqs 27−34, the pressure drop of the wellbore can be expressed as

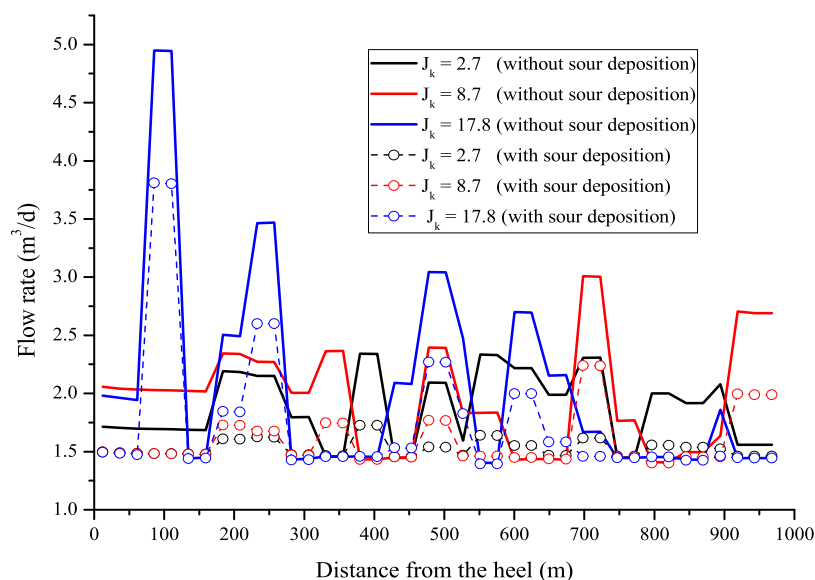**Figure 11.** Inflow profile of the horizontal well in the sulfur gas reservoir.

Figure 12. Influence of the permeability contrast.

$$p_{w,i}{}^2 - p_{w,i+1}{}^2 = 1.0 \times 10^{-6}\left(f_i \frac{16M_{air}\gamma_g p_{sc}{}^2 q_{scwi}{}^2 TZ_i}{\pi^2 RD^4 T_{sc}}L_i\right.$$

$$+ \frac{64M_{air}\gamma_g p_{sc}{}^2 q_{scwi}q_{sci}TZ_i}{\pi^2 RD^4 T_{sc}}$$

$$\left.+ \frac{32M_{air}\gamma_g p_{sc}{}^2 q_{sci}^2 TZ_i}{\pi^2 RD^4 T_{sc}}\right) \tag{35}$$

where Z_i is the deviation factor of part i.

It is to be noted that the frictional pressure drop is the first item, and the acceleration pressure drop is the second and third items.

Coupled Model and Solution. As shown in Figure 4, gas reservoir seepage and wellbore flow are coupled to study the influence of the horizontal well inflow profile in the heterogeneous sulfur gas reservoir.

For production control

$$Q_{max} = \sum_{i=1}^{n} q_i \tag{36}$$

For bottom-hole pressure control

$$p_1 = p_{wf,min} \tag{37}$$

where Q_{max} is the maximum production, m³/d and $p_{wf,min}$ is the minimum bottom hole pressure, Mpa.

The coupled model is constituted by eqs 26−37. Because the model is nonlinear, this model can be solved by the Newton Raphson method. The detailed solution process is shown in Figure 5.

RESULTS AND DISCUSSION

The effectiveness and application of the reservoir wellbore coupling model proposed in this paper are illustrated by a horizontal well of a sulfur gas reservoir. Basic parameters of the sulfur gas reservoir and horizontal well are shown in Table 1 and Figure 6. The comparison of the results is shown in Figure 7. The results of this paper model compared to the results of the model without considering the effect of sulfur deposition indicate that the new reservoir/wellbore model with sulfur deposition is better fitted to sulfur gas field data, and the average relative errors of the two simulation results are 8.37 and 23.38%, respectively. It shows that sulfur deposition in the sulfur gas reservoir is an important phenomenon that cannot be ignored.

Table 2. Distribution of Horizontal Permeability

distance from the heel [m]	permeability $[10^{-3} \ \mu m^2]$		
	$Jk = 2.7$	$Jk = 8.7$	$Jk = 17.8$
6760.3	2.601	3.179	3.05
6834.9	2.601	3.179	9.248
6894.9	2.601	3.179	1.0716
6940.9	3.468	3.757	4.046
6986.9	3.5102	3.6414	5.9245
7032.9	2.8033	3.179	0.8381
7078.9	1.9074	3.8148	1.6785
7124.9	3.757	0.8959	1.8785
7170.9	1.6005	1.6473	3.3235
7216.9	3.3235	3.8726	5.1
7262.9	2.9854	2.89	4.02
7308.9	3.5547	2.89	0.5202
7354.9	3.3524	1.6404	4.4217
7400.9	3.1501	1.1849	3.4391
7446.9	3.4969	4.9997	2.601
7492.9	2.1964	2.5744	1.445
7538.9	3.3501	0.578	2.023
7584.9	3.3056	2.312	0.8381
7630.9	3.2657	2.5432	2.89
7676.9	2.3987	4.3639	1.445
7728.3	1.3762	4.5373	0.6069

Figures 8 and 9 illustrate production changes with sulfur deposition and the inflow profile of the horizontal well, respectively. For a horizontal well with a producing pressure drop of 3 Mpa, the production decreases with increased sulfur deposition. Also, the flow rate along the horizontal well decreases because the sulfur deposition is higher, which results in a lower flow rate along the horizontal well.

Figure 10 illustrates the influence of producing pressure drop. The production both without and with sulfur deposition increases with increased producing pressure drop, while the production without sulfur deposition is higher. Figure 11 illustrates the flow rate without and with sulfur deposition along the horizontal well. The effect of sulfur deposition on the high part of the permeability is greater than that of the low part of the permeability with the increase in the production differential pressure. Also, higher producing pressure drop causes a higher nonuniform inflow profile along the horizontal well.

As shown in Table 2, the permeability of the three groups is set with different permeability contrasts (Jk). Figure 12 illustrates the bigger difference of the permeability contrast in production without and with sulfur deposition and the greater nonuniform inflow profile along the horizontal well in

heterogeneous sulfur gas reservoirs. Also, sulfur deposition can reduce the nonuniform biased inflow profile along the horizontal well in heterogeneous sulfur gas reservoirs, but the production of horizontal wells is reduced.

CONCLUSIONS

A new semianalytical model based on the volumetric source method for horizontal wells in sulfur gas reservoirs is developed. The production and the inflow performance of a horizontal well are simulated based on the new model. Compared with the results without considering the effect of sulfur deposition, the calculation results of the new reservoir/wellbore model with sulfur deposition are better fitted to sulfur gas field data, and the average relative errors of the two simulation results are 8.37% and 23.38%, respectively. Based on the model, we determine sensitivity in terms of various sulfur depositions, producing pressure drop, and permeability contrast. The results in detail are stated as follows:

(1) The production decreases with increased sulfur deposition under a certain pressure. Also, the flow rate along the horizontal well decreases because sulfur deposition is higher, which results in a lower flow rate along the horizontal well.

(2) The production without and with sulfur deposition increases with increased producing pressure drop, while the production without sulfur deposition is higher. With the increase of producing pressure drop, the effect of sulfur deposition on the high part of the permeability is greater than that of the low part of the permeability. Also, higher producing pressure drop results in a bigger nonuniform inflow profile along the horizontal well.

(3) The bigger difference of the permeability contrast in production without and with sulfur deposition and the greater nonuniform inflow profile along the horizontal well in heterogeneous sulfur gas reservoirs are illustrated. Also, sulfur deposition can reduce the nonuniform biased inflow profile along the horizontal well in heterogeneous sulfur gas reservoirs, but the production of horizontal wells is reduced.

APPENDIX[19,20]

From eqs 6−9, the characteristic equation can be expressed as

$$
\begin{cases}
\dfrac{\partial^2 E}{\partial x^2} + \dfrac{\partial^2 E}{\partial y^2} + \dfrac{\partial^2 E}{\partial z^2} = -\lambda E \\[2mm]
\dfrac{\partial E}{\partial x}\Big|_{x=0} = \dfrac{\partial E}{\partial x}\Big|_{x=x_e} = 0 \\[2mm]
\dfrac{\partial E}{\partial y}\Big|_{y=0} = \dfrac{\partial E}{\partial y}\Big|_{y=y_e} = 0 \\[2mm]
\dfrac{\partial E}{\partial z}\Big|_{z=z_e} = 0 \quad E|_{z=0} = 0
\end{cases}
\tag{A.1}
$$

Let $E = =X(x)Y(y)Z(z)$, according to separation variables, eq A.1 can be transformed as three one-dimensional eigenvalue problems

$$\begin{cases} X'' + \mu X = 0 \\ X'|_{x=0} = X'|_{x=x_e} = 0 \end{cases} \qquad \begin{cases} Y'' + \nu Y = 0 \\ Y'|_{x=0} = Y'|_{x=x_e} = 0 \end{cases}$$

$$\begin{cases} Z'' + \theta Z = 0 \\ Z'|_{z=z_e} = 0 \\ Z|_{z=0} = 0 \end{cases} \tag{A.2}$$

where

$$\lambda = \mu + \nu + \theta \tag{A.3}$$

Based on eq 16, the characteristics values of three one-dimensional eigenvalue problems are

$$\mu_l = \left(\frac{l\pi}{x_e}\right)^2, \qquad X_l = \cos\frac{l\pi}{x_e}, \ l = 0,1,2.... \tag{A.4}$$

$$\nu_l = \left(\frac{m\pi}{y_e}\right)^2, \qquad X_l = \cos\frac{m\pi}{y_e}, \ m = 0,1,2.... \tag{A.5}$$

$$\theta_n = \left(\frac{\frac{\pi}{2} + n\pi}{z_e}\right)^2, \qquad Z_n = \cos\frac{\left(\frac{\pi}{2} + n\pi\right)}{z_e}, \ n = 0,1,2.... \tag{A.6}$$

According to eqs A.4−A.6, the characteristic value of three one-dimensional eigenvalue problems is

$$\lambda = \left(\frac{l\pi}{x_e}\right)^2 + \left(\frac{m\pi}{y_e}\right)^2 + \left(\frac{\frac{\pi}{2} + n\pi}{z_e}\right)^2 \tag{A.7}$$

The corresponding characteristic function system of three one-dimensional eigenvalue problems is

$$E_{lmn}(x, y, z) = \cos\frac{l\pi}{x_e} \cos\frac{m\pi}{y_e} \sin\left(\frac{\frac{\pi}{2} + n\pi}{z_e}\right) l, \ m, \ n$$

$$= 0,1,2, \ .... \tag{A.8}$$

The 2-norm of eigen function of the characteristic function is

$$\|E_{l,m,n}(x, y, z)\|^2 = \frac{w_x w_y w_z}{8} A_l B_m \ l, \ m = 0,1,2.... \tag{A.9}$$

where

$$A_l = \begin{cases} 2 \ l = 0 \\ 1 \ l \neq 0 \end{cases} \qquad B_m = \begin{cases} 2 \ m = 0 \\ 1 \ m \neq 0 \end{cases} \tag{A.10}$$

Taking eqA.9 of the characteristic function system as transformation kernel, the model established in this paper is solved through orthogonal transformation. The corresponding orthogonal transformation can be described as follows

$$\widetilde{\psi} = G(\Delta\psi) = \int_0^{x_e} \int_0^{y_e} \int_0^{z_e} E_{l,m,n}(x, y, z)\Delta p d_x d_y d_z$$

$$l, \ m, \ n = 0,1,2.... \tag{A.11}$$

Based on eqA.9, the inverse transformation of eq 27 is as follows

$$\Delta\psi = \sum_{l=0}^{\infty}\sum_{m=0}^{\infty}\sum_{n=0}^{\infty} \frac{E_{l,m,n}(x, y, z)}{\|E_{l,m,n}(x, y, z)\|^2}\widetilde{\psi} \tag{A.12}$$

Using orthogonal transformation in eqA.12, eqs 7−11 can be converted as

$$\widetilde{\psi} = -\frac{1}{\gamma}\frac{q_{sc}pT}{86.4ke^{\alpha_{s_s}}V_{source}T_{sc}}G[h(x, y, z)] \tag{A.13}$$

Substituting eqA.13 into eqA.12, the solution of the model in this paper is

$$\Delta\Psi = G(\Delta\psi) = \sum_{l=0}^{\infty}\sum_{m=0}^{\infty}\sum_{n=0}^{\infty}\frac{1}{\gamma}\frac{q_{sc}pT}{86.4ke^{\alpha_{s_s}}V_{source}T_{sc}}$$

$$\frac{-E_{l,m,n}(x, y, z)G[h(x, y, z)]}{\|E_{l,m,n}(x, y, z)\|^2} = \frac{q_{sc}pT}{86.4ke^{\alpha_{s_s}}V_{source}T_{sc}}$$

$$\sum_{l=0}^{\infty}\sum_{m=0}^{\infty}\sum_{n=0}^{\infty}\frac{\sigma_l(x)\sigma_m(y)\sigma_n(z)}{\gamma} \tag{A.14}$$

where

$$\sigma_l(x) = \begin{cases} \dfrac{2w_x}{x_e} & l = 0 \\[4mm] \dfrac{4\cos\frac{l\pi x}{x_e}\cos\frac{l\pi c_x}{x_e}\sin\frac{l\pi w_x}{x_e}}{l\pi} & l \neq 0 \end{cases} \tag{A.15}$$

$$\sigma_m(y) = \begin{cases} \dfrac{2w_y}{y_e} & m = 0 \\[4mm] \dfrac{4\cos\frac{m\pi y}{y_e}\cos\frac{m\pi c_y}{y_e}\sin\frac{m\pi w_y}{y_e}}{m\pi} & m \neq 0 \end{cases} \tag{A.16}$$

$$\sigma_n(z) = \frac{4\sin\frac{\left(\frac{\pi}{2} + n\pi\right)z}{z_e}\cos\frac{\left(\frac{\pi}{2} + n\pi\right)c_z}{z_e}\sin\frac{\left(\frac{\pi}{2} + n\pi\right)w_z}{z_e}}{n\pi} n = 0,1,2... \tag{A.17}$$

■ AUTHOR INFORMATION

Corresponding Author

Ting Li − *Petroleum Engineering College, Yangtze University, Wuhan 430100, China; State Key Laboratory of Petroleum Resources and Prospecting, China University of Petroleum, Beijing 102249, China;* orcid.org/0000-0002-4970-8144; Email: 2695377412@qq.com

Authors

Mingren Shao − *China United Coalbed Methane Corporation, Ltd., Beijing 100011, China*

Qi Yang − *China United Coalbed Methane Corporation, Ltd., Beijing 100011, China*

Bo Zhou − *Downhole Technology Operation Company, CNPC Chuanqing Drilling Engineering Company Limited, Xi'an 710021, Shanxi, China*

Shuhui Dai − *Exploration and Development Department, China ZhenHua Oil Co., Ltd., Beijing 100031, China*

Faraj Ahmad − *Petroleum Engineering Department, Colorado School of Mines, Golden, Colorado 80401, United States*

Complete contact information is available at:
https://pubs.acs.org/10.1021/acsomega.0c06143

REFERENCES

(1) Al-Majed, M. A. New model to predict formation damage due to sulfur deposition in sour gas wells. *SPE North Africa Technical Conference and Exhibition, Cairo, Egypt*, 2012.

(2) Guo, X.; Zhou, X.; Zhou, B. Prediction model of sulfur saturation considering the effects of non-Darcy flow and reservoir compaction. *J. Nat. Gas Sci. Eng.* **2015**, *22*, 371−376.

(3) Hu, J.-H.; He, S.-L.; Zhao, J.-Z.; Li, Y.-M.; Yang, X.-F. Sulfur deposition experiment in the presence of non-movable water. *J. Pet. Sci. Eng.* **2012**, *100*, 37−40.

(4) Hu, J.-H.; He, S.-L.; Zhao, J.-Z.; Li, Y.-M.; Deng, Y. Modeling of Sulfur Deposition Damage in the Presence of Irreducible Water. *Pet. Sci. Technol.* **2011**, *29*, 499−505.

(5) Kennedy, H. T.; Wieland, D. R. Equilibrium in the methane-carbon dioxide-hydrogen sulfide-sulfur system. *Soc. Pet. Eng. J.* **1960**, *219*, 166−169.

(6) Mahmoud, M. A. A. Effect of elemental-sulfur deposition on the rock petrophysical properties in sour-gas reservoirs. *SPE J.* **2014**, *19*, 703−715.

(7) Abou-Kassem, J. H. Experimental and numerical modeling of sulfur plugging in carbonate reservoirs. *J. Petrol. Sci. Eng.* **2000**, *26*, 91−103.

(8) Mei, H.; Zhang, M.; Yang, X. The effect of sulfur deposition on gas deliverability. *SPE Gas Technology Symposium, Calgary, Alberta, Canada*, 2006.

(9) Roberts, B. E. The effect of sulfur deposition on gas well inflow performance. *SPE Reservoir Eng.* **1997**, *12*, 118−123.

(10) Li, T.; Tan, Y.; Ahmad, F. A.; Zhao, J. Experimental study of sand distribution among perforation clusters in horizontal wellbore of shale gas reservoir. *J. Chem.* **2020**, *2020*, 1−7.

(11) Li, T.; Tan, Y.; Ahmad, F. A.; Liu, H. A new method to production prediction for the shale gas reservoir. *Energy Sources, Part A* **2020**, *6*, 615−622, DOI: 10.1080/15567036.2020.1779876.

(12) Li, T., Tan, Y., Dai, S., Zhou, X., Yu, J., Yang, Q. Semi-analytical model based on the volumetric source method to production simulation from nonplanar fracture geometry in tight oil reservoirs. *ACS Omega* **2020**, *6*DOI: DOI: 10.1021/acsomega.0c05119.

(13) Kou, Z.; Dejam, M. Dispersion due to combined pressure-driven and electro-osmotic flows in a channel surrounded by a permeable porous medium. *Phys. Fluids* **2019**, *31*, 056603.

(14) Kou, Z.; Dejam, M. Control of shear dispersion by the permeable porous wall of a capillary tube. *Chem. Eng. Technol.* **2020**, *43*, 2208−2214.

(15) Penmatcha, V. R.; Aziz, K. A comprehensive reservoir/wellbore model for horizontal wells. *SPE J.* **1998**, *4*, 224−234.

(16) Ozkan, E.; Sarica, C.; Haci, M. Influence of pressure drop along the wellbore on horizontal-well productivity. *SPE J.* **1999**, *4*, 288−301.

(17) Zhang, L.; Kou, Z.; Wang, H.; Zhao, Y.; Dejam, M.; Guo, J.; Du, J. Performance analysis for a model of a multi-wing hydraulically fractured vertical well in a coalbed methane gas reservoir. *J. Petrol. Sci. Eng.* **2018**, *166*, 104−120.

(18) Kou, Z.; Wang, H. Transient pressure analysis of a multiple fractured well in a stress-sensitive coal seam gas reservoir. *Energies* **2020**, *13*, 3849.

(19) Wang, H.; Kou, Z.; Guo, J.; Chen, Z. A semi-analytical model for the transient pressure behaviors of a multiple fractured well in a coal seam gas reservoir. *J. Petrol. Sci. Eng.* **2021**, *198*, 108159.

(20) Valkó, P. P.; Amini, S. The method of distributed volumetric sources for calculating the transient and pseudosteady-state productivity of complex well-fracture configurations. *SPE Hydraulic Fracturing Technology Conference, College Station, Texas, U.S.A.*, 2007.

(21) Vicente, R.; Sarica, C.; Ertekin, T. A numerical model coupling reservoir and horizontal well flow dynamics: Transient behavior of single-phase liquid and gas flow. *SPE J.* **2002**, *7*, 70−77.

(22) Ouyang, L.; Huang, W. A comprehensive evaluation of well-completion impacts on the performance of horizontal and multilateral wells. *SPE Annual Technical Conference and Exhibition, Dallas, Texas*, 2005.

(23) Karimifard, M.; Durlofsky, L. J. An expanded well model for accurate simulation of reservoir-well interactions. *ECMOR XII-12th European Conference on the Mathematics of Oil Recovery*, 2010.

(24) Souza, G. D.; Pires, A. P.; Abreu, E. Well-reservoir coupling on the numerical simulation of horizontal wells in gas reservoirs. *SPE Latin America and Caribbean Petroleum Engineering Conference, Maracaibo, Venezuela*, 2014.

(25) Luo, W.; Li, H.-T.; Wang, Y.-Q.; Wang, J.-C. A new semi-analytical model for predicting the performance of horizontal wells completed by inflow control devices in bottom-water reservoirs. *J. Nat. Gas Sci. Eng.* **2015**, *27*, 1328−1339.

(26) Tan, Y.; Li, Q.; Li, H.; Zhou, X.; Jiang, B. A semi-analytical model based on the volumetric source method to predict acid injection profiles of horizontal wells in carbonate reservoirs. *J. Energy Resour. Technol.* **2020**, *143*, 053001.

(27) Li, H.; Tan, Y.; Jiang, B.; Wang, Y.; Zhang, N. A semi-analytical model for predicting inflow profile of horizontal wells in bottom-water gas reservoir. *J. Pet. Sci. Eng.* **2018**, *160*, 351−362.

(28) Tan, Y.; Li, H.; Zhou, X.; Jiang, B.; Wang, Y.; Zhang, N. A semi-analytical model for predicting horizontal well performances in fractured gas reservoirs with bottom-water and different fracture intensity. *J. Energy Resour. Technol.* **2018**, *140*, 102905.

(29) Adesina, A. P.; Orodu, O.; Oladepo, A. An improved model for estimating productivity of horizontal drain hole. *SPE Nigeria Annual International Conference and Exhibition, Lagos, Nigeria*, 2016.

(30) Ping, Z.; Zhao, J.; Zhou, H. Formation damage from elemental sulfur deposition in sour gas reservoir. *Pet. Explor. Dev.* **2005**, *32*, 113−115.

(31) Wolfsteiner, C.; Durlofsky, L. J.; Khalid, A. Approximate model for productivity of nonconventional wells in heterogeneous reservoirs. *SPE J.* **2000**, *5*, 218−226.

(32) Hawkins, M. F. A Note on the Skin Effect. *J. Pet. Technol.* **1956**, *8*, 65−66.

(33) Sun, E.; Li, X. Study on horizontal wellbore pressure of low permeability reservoirs. *Reservoir Eval. Dev.* **2013**, *3*, 38−40.